Steering Liquid Pt-Si Nanodroplets on Si(100) by Interactions with Surface Steps

P. Sutter,[1,*] P. A. Bennett,[2] J. I. Flege,[1] and E. Sutter[1]

[1]*Center for Functional Nanomaterials, Brookhaven National Laboratory, Upton, New York 11973, USA*
[2]*Department of Physics and School of Materials, Arizona State University, Tempe, Arizona 85287, USA*

(Received 22 April 2007; published 20 September 2007)

Liquid eutectic Pt-Si droplets, migrating across a Si(100) surface due to an applied temperature gradient, interact measurably with surface steps. An analysis of the interaction yields a critical size of hundreds of nanometers below which droplets are constrained to move parallel to monolayer steps. Bunches of closely spaced steps are capable of guiding larger, micron-sized droplets. This steering by steps or step bunches may be used for the controlled manipulation of liquid droplets on patterned surfaces, and affects fundamental surface processes such as coarsening.

DOI: 10.1103/PhysRevLett.99.125504 PACS numbers: 61.46.−w, 68.37.Nq

The widespread use of nanomaterial synthesis techniques such as vapor-liquid-solid growth [1], which employs a liquid binary eutectic as a seed and driver of the growth of semiconductor nanowires, has sparked interest in the properties of surface-supported eutectic droplets. Given the need for placement control in arrays of self-assembled nanostructures [2], methods for achieving long-range ordered arrangements of eutectic seeds as a template for ordered nanowire arrays become particularly important. Ideally, minimal top-down (lithographic) intervention should be required to induce such ordering, using pattern feature sizes well above the characteristic length scale of the nanoscale objects.

Liquid binary eutectics have been shown to undergo spontaneous thermomigration. The migration of liquid inclusions in bulk materials with an applied temperature gradient ∇T has been studied extensively, particularly for Si-based alloys with deep eutectic points (Al-Si, Au-Si) in a Si matrix [3,4]. The migration trajectories follow the (local) ∇T toward higher temperature, and in a diffusion-limited regime the velocity depends exponentially on temperature [3]. Recently, we [5] and others [6] have demonstrated the migration of sub-μm and μm-sized Pt-Si droplets on silicon surfaces, governed by the same physical principles as thermomigration in the bulk. Such surface thermomigration can be viewed as a parasitic effect, as it may both randomize the placement and alter the size distribution (via coalescence) of groups of eutectic droplets. On the other hand, spontaneous migration could provide an elegant way of positioning nanoscale liquid droplets if suitable interactions with externally defined morphological patterns, such as appropriate arrangements of surface steps, are identified that can be used to steer droplet motion. Here we use time-resolved surface microscopy at high temperatures to identify and quantify a fundamental droplet-step interaction for a particular model system, Pt-Si/Si(100). While the interaction strength may differ somewhat for other systems, the underlying physics and its implications, e.g., for droplet organization, are general and apply broadly to liquid alloy droplets interacting with surface steps.

To observe migrating Pt-Si droplets and steps simultaneously, we used bright-field low-energy electron microscopy (LEEM) with 10 nm lateral resolution and acquisition rates of up to 10 images per second. Under slightly off-normal illumination, Si(100) (2×1) and (1×2) reconstruction domains are imaged as alternating dark and bright areas whose boundaries mark the positions of atomic surface steps. Si(100) samples (miscut $<0.1°$) were cleaned by repeated flashing to 1200 °C. Evaporation of about 10 monolayers (ML) Pt at 800 °C followed by annealing above the bulk eutectic point (980 °C) produced liquid Pt-Si droplets with initial diameters below 100 nm on the surface. Larger droplets were spontaneously generated by coalescence. A temperature gradient due to localized electron-beam heating of the sample center was used to drive the surface thermomigration of these Pt-Si droplets. The temperature profile was determined from a three-color image of the glowing sample, calibrated by matching the brightness at the center to pyrometer readings for a series of temperatures.

Figure 1 shows the trajectories and time-dependent velocities of several migrating Pt-Si droplets at $T = 1100$ °C. Large droplets (#1, #2; radii: $r_1 = 640$ nm, $r_2 = 500$ nm) move—as expected—with constant speed [~ 200 nm/s, Fig. 1(b)] on straight paths aligned with the local ∇T [3]. Somewhat smaller droplets (#3; $r_3 = 380$ nm) deviate from this behavior, e.g., can become completely immobilized for extended time periods. The trajectories of the smallest droplets (#4, #5; $r_4 = 180$ nm, $r_5 = 120$ nm) are not straight, but consist of curved segments that only approximately align with the paths of the large drops (i.e., ∇T). Substantial variations in droplet speed are observed [Fig. 1(b)]. The individual trajectories are closely aligned with surface steps, suggesting the presence of a droplet-step interaction that could become the basis for steering the migration.

We have used sequences of LEEM images to identify and quantitatively analyze this interaction for droplets of different sizes crossing individual surface steps (Fig. 2) as well as step bunches (Fig. 4). The fundamental droplet-step interaction, the pinning of surface steps by the migrating

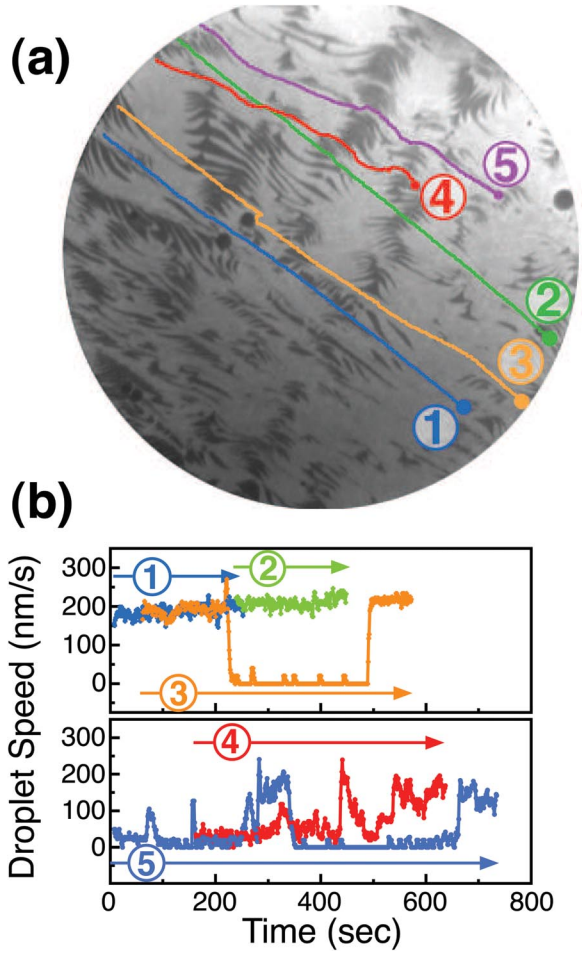

FIG. 1 (color). (a) Bright-field LEEM image (field of view 50 μm) of Si(100) with migrating Pt-Si droplets. Dark and bright areas are (2×1) and (1×2) reconstructed domains separated by atomic steps. Lines mark trajectories of Pt-Si droplets (traced from a LEEM movie), driven by a temperature gradient from lower right (cold) to upper left (hot). (b) Time-dependent speed of the Pt-Si droplets in (a). The slow increase in speed of particle 1 is due to a slight rise in sample temperature.

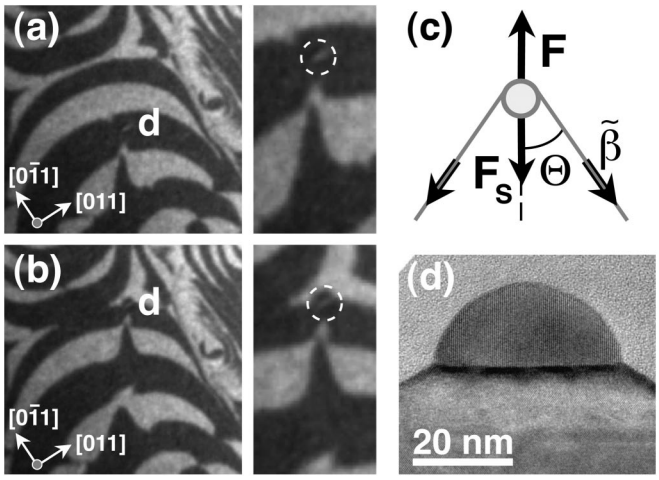

FIG. 2. (a),(b) Bright-field LEEM images of the pinning of individual atomic steps by a migrating Pt-Si droplet (d). Left—overview (field of view 14 μm); right—high magnification view of the step pinning. Dashed circles—Pt-Si droplet (c) Schematic representation of the forces acting on a pinned droplet: F—driving force for migration; F_S—retarding force due to step line tension $\tilde{\beta}$. (d) Cross-sectional transmission electron micrograph of a Pt-Si particle after cooling to room temperature, showing a planar Pt-Si/Si(100) interface.

droplets, is illustrated in Figs. 2(a) and 2(b). As a larger ($r \approx 500$ nm) droplet crosses single steps that are roughly perpendicular to its trajectory, step pinning causes a dragging of the ledges [7]. Only when this deformation reaches a certain threshold, the droplet breaks free and the step relaxes back to its original straight configuration. The depinning is a consequence of the stiffness (or line tension) $\tilde{\beta}$ of the surface step, the free-energy cost per unit length of bending a step edge [8]. It occurs as the step deformation reaches an angle Θ at which the net force due to the line tension $F_s = 2\tilde{\beta}\cos\Theta$ reaches the maximum pinning force $F_s^{\max}$ due to the microscopic wetting interaction between droplet and step [Fig. 2(c)]. $F_s^{\max}$ can therefore be determined from LEEM observations such as Figs. 2(a) and 2(b), and the step stiffness. The maximum deformation differs for alternating steps, reflecting differences in stiffness between the two types of atomic steps, S_A and S_B, on Si(100) [9]. For steps with predominant S_B character, we measure a depinning angle $\Theta \approx 10°$. Further LEEM experiments suggest that fundamental step properties, such as the stiffness, are unaffected by the presence of Pt, so that known $\tilde{\beta}$ values for clean Si(100) can be used to quantify the droplet-step interaction. With $\tilde{\beta}(S_B) = 10$ meV/nm at 1100 °C [9], we find $F_s^{\max} \approx 3\times10^{-12}$ N.

The migration trajectory and speed of large droplets crossing perpendicular to single steps, as in Fig. 2, are only slightly influenced by step pinning. Smaller drops and drops crossing at shallower angles are affected more strongly, to the point of being immobilized [normal incidence, Fig. 3(a)] or following along the step edge [grazing incidence, Fig. 3(b)]. Using the maximum pinning force derived above we can estimate the droplet radius r_c, below which step crossing is suppressed. When a droplet of radius r_c moving perpendicular to a step is just immobilized, the driving force F of the droplet migration (which depends on droplet size) is balanced by $F_s^{\max}$ (assumed size independent) [Fig. 3(a)]. F, due to the dissolution of Si at the leading (high T) edge of a droplet and its redeposition at the trailing edge, can be estimated from the free-energy change dE per volume dV of transported Si [10], $dE = \delta\tilde{S}\Delta T dV$, where $\delta\tilde{S}$ denotes the specific entropy of fusion of Si, and $\Delta T = \frac{\partial T}{\partial x}\sqrt{2}r$ is the temperature difference across the droplet (radius r), given an overall temperature gradient $\frac{\partial T}{\partial x}$ [11]. For an infinitesimal migration step dx, $dV \approx \sqrt{2}rhdx$, where h is the depth to which Si is dissolved into the droplet. The driving force for migration hence becomes $|F| = \frac{dE}{dx} \approx \delta\tilde{S}\frac{\partial T}{\partial x}2r^2h$.

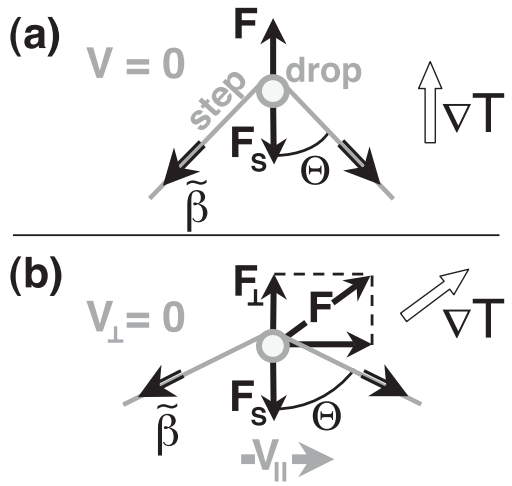

FIG. 3. Schematic representation of the force balance of a migrating droplet interacting with an atomic surface step. (a) Normal incidence—immobilization. (b) Grazing incidence—steering along the step. Symbols are explained in the text.

Equating F to the maximum pinning force $F_s^{\max}$, with $\delta\tilde{S} = 30\ \mathrm{J\,mol^{-1}\,K^{-1}}$ [12] and $\frac{\partial T}{\partial x} = 3 \times 10^4\ \mathrm{K\,m^{-1}}$ [5], and estimating Si dissolution limited to the topmost 3 ML beneath the leading edge of the droplet ($h = 0.4$ nm), we find a critical radius $r_c = \sqrt{F_S^{\max}/[2h\delta\tilde{S}(\partial T/\partial x)]} \cong 200$ nm. Droplets with radius $r \leq r_c$ are expected to be immobilized completely when attempting to cross perpendicular to a step at 1100 °C. This analysis suggests that the migration of large droplets, hundreds of nanometers in size, can be strongly affected by individual atomic steps on Si(100), in excellent agreement with the LEEM observations of Fig. 1.

Perpendicular step crossing [Fig. 3(a)] is a special case, and most migrating droplets will encounter steps at shallower angles [Fig. 3(b)]. Step drag will then cancel the droplet velocity component perpendicular to the step—and the droplet will follow along the step edge instead of crossing it—if the projected driving force $F_\perp$ equals the maximum holding force $F_s^{\max}$ of the step. Hence, droplets with larger radius than estimated above can be guided along an atomic step if the angle between ∇T and the step is small. Finally, in addition to single steps, step bunches exist on many crystalline surfaces. The wetting interaction between a drop and a N-step bunch is roughly N times that of a single step, i.e., $F_s^{\max} \propto N$. A N-step bunch hence will hold or guide droplets with $\sqrt{N}$ larger radius than a single step. The possibility to form step bunches allows extending the concepts of droplet-step interactions and steering from nanometer to micrometer droplet sizes.

The steering of larger Pt-Si droplets on trajectories away from the thermal gradient is shown in Fig. 4. The narrow, curved dark band running from upper left to lower right is a bunch of about 10–15 steps, as confirmed by atomic force microscopy. Several droplets (e.g., #1–#3), observed in

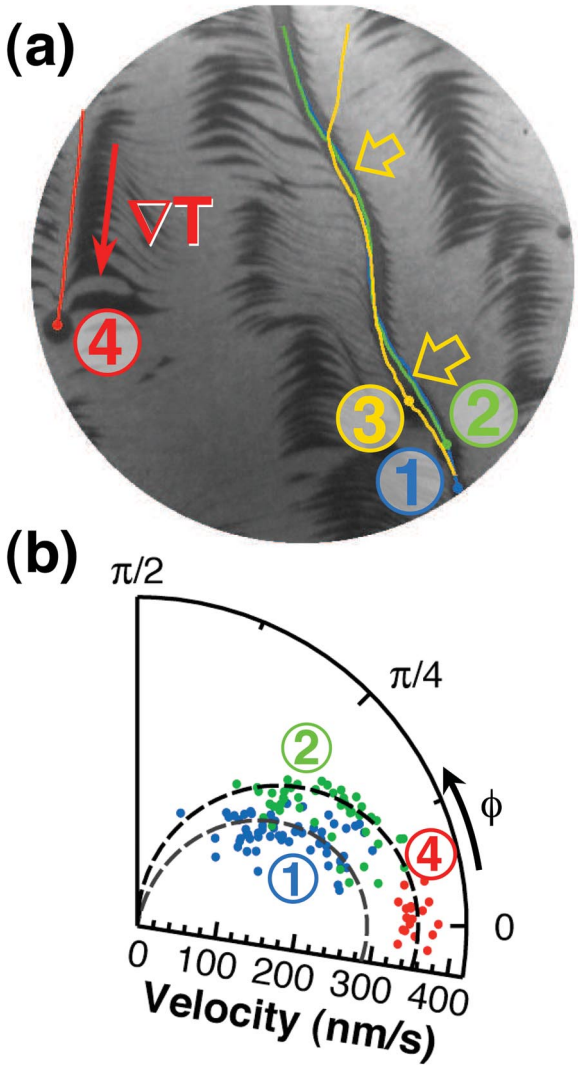

FIG. 4 (color). (a) Bright-field LEEM image and overlaid trajectories of Pt-Si droplets guided by a step bunch on Si(100) [#1–#3], and of one free droplet marking the direction of ∇T [#4]. (b) Polar diagram of the migration speed as a function of the angle ϕ between droplet trajectory and ∇T. Dashed lines are fits of $V_\parallel = V_0 \cos(\phi) - \Delta$ to the data, assuming $\Delta = 0$ (outer) and $\Delta > 0$ (inner).

short sequence to ensure constant T and ∇T, are guided by the step bunch. Other large droplets (e.g., #4), moving freely in adjacent areas with low step density, mark the direction of the local temperature gradient. LEEM observations show droplets with radii of several hundred nm guided by the step bunch, which is deformed little due to the considerable stiffness of an N-step bunch (N times that of a single step [13]). Droplets #1 and #2 ($r_1 = 200$ nm, $r_2 = 350$ nm) experience a normal drag force sufficient to steer them significantly away from the local ∇T. They move on identical trajectories along the step bunch. Even larger particles ($r = 580$ nm) remain guided as long as the step bunch is closely aligned with ∇T, but leave the track when it deviates too strongly from the direction of ∇T, i.e., when the driving force for migration perpendicular to the

step bunch becomes larger than the maximum holding force of the bunch. Droplet #3 ($r_3 = 480$ nm) represents an intermediate case. Although it remains pinned to the step bunch, its trajectory deviates measurably from those of the two smaller droplets (#1, #2) in sections of the track with large angle to ∇T, but perfectly matches the other two trajectories in sections that align closely with ∇T.

Movies of the migration of several droplets (100 to 500 nm radius) along the step bunch in Fig. 4(a) provide the opportunity of probing the effects of steering on migration speed. The droplet speed should vary with the projection of ∇T onto the track, i.e.,$V_{\parallel} = V_0 \cos(\phi)$, where ϕ is the (local) angle between the step bunch and ∇T. Combining observations of unguided droplets and of those steered along the step bunch, we determined the migration speed up to angles ϕ of about $\pi/4$ [Fig. 4(b)]. We find a very close agreement with the expected cosine dependence, at least for larger droplets (#2). Smaller particles (#1) show measurably lower speeds, likely because the droplets cross steps periodically during their motion along the step bunch. This causes drag in the direction of motion and reduces the droplet speed by a constant Δ, so that $V_{\parallel} = V_0 \cos(\phi) - \Delta$. Because of the same effect, very small droplets (not shown here) become completely immobilized once they enter the track from the sides.

The fact that the thermomigration of liquid droplets can be steered by step bunches suggests a practical approach to control the positioning of nanoscale eutectic drops using lithographically established step patterns, consisting of straight sections with small ϕ (guiding droplet motion) and sharp corners with large ϕ (immobilizing the droplets). Indeed, such a mechanism may explain an earlier demonstration of alignment of Au-Si islands on patterned Si surfaces [14,15], loosely interpreted as being due to the accumulation of liquid metal at an ''energetically stable position'' on the patterned surface. Our results suggest that liquid Au-Si droplets above the eutectic temperature could instead have been propelled by thermal gradients, steered, and ultimately immobilized by the surface step patterns.

In addition to the controlled placement of liquid alloy droplets, achievable by thermomigration on patterned surfaces, control over particle size is a second key requirement in nanotechnology. At least two primary processes affect the size of individual particles in an array: Ostwald ripening and coalescence. Ripening is a consequence of the increase of the chemical potential with curvature, which leads to the net dissolution of smaller and growth of larger particles. Coalescence typically depends less on size but requires the ''collision'' of particles [16]. The size-dependent retardation in step bunches gives rise to a coalescence mechanism in which large droplets moving at high speed absorb smaller, slower droplets, which—similar to ripening—leads to the growth of larger particles at the expense of smaller ones. The presence of one-dimensional tracks capturing and guiding migrating droplets increases the probability of coalescence events compared to random motion on a flat surface.

In future work, time-resolved surface imaging, used here to detect and quantify the interaction of migrating Pt-Si alloy droplets with surface steps, can be used to resolve remaining open questions, e.g., regarding the detailed interaction mechanism. Synchrotron photoemission microscopy will provide important complementary information on the distribution of the alloy components on the substrate surface.

Work carried out under the auspices of the U.S. Department of Energy under Contract No. DE-AC02-98CH1-886 and supported by NSF NIRT Grant No. ECS-0304682.

*Corresponding author.
psutter@bnl.gov

[1] A. M. Morales and C. M. Lieber, Science **279**, 208 (1998).
[2] See, e.g., C. Thelander, P. Agarwal, S. Brongersma, J. Eymery, L. F. Feiner, A. Forchel, M. Scheffler, W. Riess, B. J. Ohlsson, U. Gösele, and L. Samuelson, Mater. Today **9**, 28 (2006).
[3] T. R. Anthony and H. E. Cline, J. Appl. Phys. **43**, 2473 (1972).
[4] H. E. Cline and T. R. Anthony, J. Appl. Phys. **47**, 2325 (1976).
[5] P. A. Bennett, J. I. Flege, P. Sutter, and E. Sutter, Phys. Rev. B (to be published).
[6] W.-C. Yang, H. Ade, and R. J. Nemanich, Phys. Rev. B **69**, 045421 (2004).
[7] J. S. Ozcomert, W. W. Pai, N. C. Bartelt, and J. E. Reutt-Robey, Surf. Sci. **293**, 183 (1993).
[8] N. C. Bartelt, R. M. Tromp, and E. D. Williams, Phys. Rev. Lett. **73**, 1656 (1994).
[9] N. C. Bartelt and R. M. Tromp, Phys. Rev. B **54**, 11 731 (1996).
[10] R. D. Doherty and T. R. Strutt, J. Mater. Sci. Lett. **11**, 2169 (1976).
[11] In the following, we approximate the circular footprint of the droplet by an inscribed square of length $a = \sqrt{2}r$, and assume a planar liquid solid interface, as observed in cross-sectional transmission electron micrographs of droplets cooled to room temperature [Fig. 2(d)].
[12] K. Yamaguchi and K. Itagaki, J. Therm. Anal. Calorim. **69**, 1059 (2002).
[13] K. Sudoh, T. Yoshinobu, H. Iwasaki, and E. D. Williams, Phys. Rev. Lett. **80**, 5152 (1998).
[14] Y. Homma, P. Finnie, and T. Ogino, Appl. Phys. Lett. **74**, 815 (1999).
[15] Y. Homma, P. Finnie, T. Ogino, H. Noda, and T. Urisu, J. Appl. Phys. **86**, 3083 (1999).
[16] More complex scenarios for coalescence have been identified as well, see E. Sutter, P. Sutter, and Y. Zhu, Nano Lett. **5**, 2092 (2005); W.-C. Yang, M. Zeman, H. Ade, and R. J. Nemanich, Phys. Rev. Lett. **90**, 136102 (2003).